Backhaul-Constrained Coverage Analysis of Integrated High and Low Altitude Platforms Aerial Communication System in Post-Disaster Areas

Yikun Zhao, Fanqin Zhou, Lei Feng, Wenjing Li, Yao Sun, and Muhammad Ali Imran

***Abstract*—Coverage analysis of aerial communication networks based on high altitude platforms (HAPs) and low altitude platforms (LAPs) is of great significance to understand the service provisioning capability of aerial base stations. This letter uses stochastic geometry to analyze network coverage of an integrated HAP and LAP (IHL) system with respect to backhaul constraints, where LAPs aim to provide services for ground user equipments in the malfunction area and a HAP is to provide backhaul connectivity for LAPs. Based on stochastic geometry theory, the analytical framework of the IHL system coverage is derived along with the analysis on the impact of some key parameters, such as aerial platform altitudes and LAP densities. The derived analytical framework can also provide insights for the backhaul design of LAP aerial base stations, which is also revealed in the numerical analyses part.**

***Index Terms*—Aerial communication networks; high altitude platforms; stochastic geometry.**

I. Introduction

SINCE wireless networks need to be swiftly deployed after a disaster strikes to provide emergency response, low altitude platforms (LAPs) are considered as a promising option for recovering wireless communication in post-disaster environments [1]. The backhaul of LAPs is mainly based on the ground infrastructure, which makes it impossible to establish backhaul connections in areas where ground infrastructure is not available. In this case, some researches propose to use satellites as the backhaul relay of LAPs to help users access the core network in catastrophic situations [2]. Recently, high altitude platform (HAP) has rekindled the interest of academia and industry and been expected to become another powerful candidate to assist LAPs by exploiting mmWave backhaul links [3]. Compared with satellites, HAP can maintain quasi-stationary in the air, which greatly eases the difficulty of beam alignment; the deployment complexity of HAP is lower, making it more suitable for emergency response; HAP's proximity to the ground also brings less path loss and lower delay.

Manuscript received xx xx, 20xx; revised xx xx, 20xx. This work was funded by the National Natural Science Foundation of China (No. 61971053) and BUPT Excellent Ph.D. Students Foundation (No. CX2022223). *Corresponding author: Fanqin Zhou, Wenjing Li.*

Yikun Zhao, Fanqin Zhou, Lei Feng and Wenjing Li are with the State Key Laboratory of Networking and Switching Technology, Beijing University of Posts and Telecommunications, Beijing, China (e-mail:yizhao@bupt.edu.cn, fqzhou2012@bupt.edu.cn, fenglei@bupt.edu.cn, wjli@bupt.edu.cn). Yao Sun and Muhammad Ali Imran are with James Watt School of Engineering, University of Glasgow, United Kingdom (e-mail: yao.sun@glasgow.ac.uk, muhammad.imran@glasgow.ac.uk).

Many recent forward-looking surveys have described the architecture and application scenarios of integrated high and low altitude platforms (IHL) system in future wireless networks [3]–[5]. HAPs' prominent attributes include long flight endurance and wide coverage, and LAPs can be deployed rapidly and move freely to obtain high line-of-sight (LoS) connections with low expenditures [4]. The IHL system can be used for providing communication service to regions where terrestrial infrastructure or LAPs alone may fail to meet coverage requirements [6]. Several works have focused on network optimization in this system, such as computation offloading [7], deployment design [8], [9] and resource allocation [9], [10]. However, current literature mainly elaborates on IHL architectures and solves a specific optimization problem, but lacks theoretical performance analyses of the IHL system.

Stochastic geometry is an effective tool to perform system-level analysis of aerial networks by employing a tractable mathematical framework. However, analyzing the coverage performance of the IHL system remains relatively unexplored. Reference [6] derived the association probability and cell load of the network where HAPs and LAPs serve ground user equipment (GUE) as macrocells and femtocells respectively, but it did not take the impact of fading into consideration in the model. Moreover, it did not focus on the backhaul issue under this architecture. In [11], the authors mentioned that the wireless backhaul connectivity for the LAPs was provided by HAPs, but they did not consider the impact of backhaul link on the coverage performance. In fact, as pointed out in [12], most existing studies limit the scope of their analyses to the access link and thus assume ideal backhaul, which may lead to an over-optimistic estimation of network performance.

Contributions: This letter develops an analytical framework based on stochastic geometry, to analyze the coverage performance of an IHL system which serves GUE in a large post-disaster malfunction area. The proposed coverage analytical framework considers not only the successful access probability but also the backhaul probability. Particularly, the coverage performance of two backhaul schemes, HAP-assisted backhaul and LAP direct backhaul, are discussed. Using the proposed analytical framework, we analyze the impact of various parameters including the altitude and intensity of the LAP layer. Through the analyses, some insights on the LAP backhaul design are also given, which may guide the performance optimization of the IHL system.

II. System Model

In this letter, we consider a terrestrial network where the ground base stations (GBSs) are independently distributed according to a homogeneous Poisson point process (PPP) Φ_g of density λ_g. Particularly, there is a circular post-disaster area D_d with radius r_d where the GBSs are unavailable for a long period of time. Without loss of generality, the center of the disc D_d is at the origin. In our proposed scheme, a HAP and several LAPs are employed together to provide communication service in the emergency. LAPs serve the GUE in the malfunction area and all the LAPs transmit at the same power P_{t_l} to GUE. Frequency division multiplexing is used between cells, and frequency division multiple access is used within a cell. This paper discusses two backhaul schemes: HAP-assisted backhaul (HAB) and LAP direct backhaul (LDB). In the HAB scheme, LAPs utilize mmWave to backhaul to the ground network through HAP, while in the LDB scheme, LAPs directly establish a mmWave backhaul link with the ground. The HAP hovers at altitude h_h above the center of disc D_d and LAPs are distributed according to a homogeneous PPP Φ_l of intensity λ_l with a fixed altitude h_l. The distribution of GUEs also follows a homogeneous PPP and our analysis is conducted at a typical GUE u_o located at the origin. This letter focuses on the backhaul-constrained coverage performance in the malfunction area D_d and an illustration of the network model is presented in Fig.1.

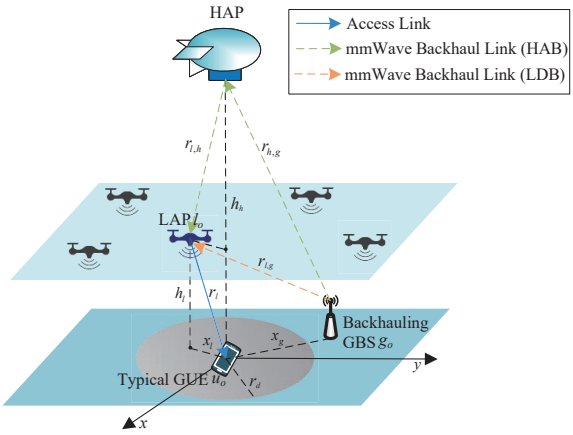

Fig. 1. The proposed system model.

A. Channel Model

1) LAP-GUE Access Link: The links between the LAPs and GUEs can be LoS or NLoS and the LoS probability is given as $P_L(x) = 1/\left(1 + a\exp\left(-b\left[\frac{180}{\pi}\arctan\left(h_l/x\right) - a\right]\right)\right)$, where a and b are environment constants and x denotes the horizontal distance between the GUE and the serving LAP. The NLoS probability is $P_N(x) = 1 - P_L(x)$. We characterize the LAP-GUE channel by a distance-dependent path loss and a small-scale Nakagami-m fading. Different path loss exponent (PLE) $\alpha_{l,L}, \alpha_{l,N}$ and fading parameters $m_{l,L}, m_{l,N}$ are modeled for the LoS and NLoS links respectively. The power received at the typical GUE from the i-th LAP is $P_{r_{l_i}} = P_{t_l} r_{l_i}^{-\alpha_{l,\zeta}} \Omega_{l_i,\zeta}, \zeta \in \{L, N\}$, where r_{l_i} is the distance from the typical GUE u to the i-th LAP, $\Omega_{l_i,\zeta}$ is the Nakagami-m fading gain of the i-th LoS/NLoS LAP which follows a Gamma distribution with the shape parameter $m_{l,\zeta}$.

2) HAP-LAP mmWave Backhaul Link: The power received at the i-th LAP from the HAP is $P_{r_{l_i,h}} = P_{t_h} C_h G_{t_h} G_{r_l} r_{l_i,h}^{-\alpha_h} \Omega_{l_i,h}$, where P_{t_h} is the transmit power of HAP on the backhaul link, G_{t_h} and G_{r_l} are the directional gain of mmWave antenna of the HAP transmitter and LAP receiver respectively, C_h and α_h are the path loss intercept and PLE of the HAP-LAP link respectively, $r_{l_i,h}$ denotes the distance from the i-th LAP to the HAP, and $\Omega_{l_i,h}$ represents the Nakagami-m fading gain between the i-th LAP and HAP.

3) GBS-HAP mmWave Backhaul Link: The received power at the HAP from the j-th GBS is $P_{r_{h,g_j}} = P_{t_g} C_{g,L} G_{t_g} G_{r_h} r_{h,g_j}^{-\alpha_{g,L}} \Omega_{h,g_j}$, where P_{t_g} is the transmit power of GBS, G_{t_g} and G_{r_h} are the mmWave directional gain of the GBS transmitter and HAP receiver, C_g and α_g are the path loss intercept and PLE of the GBS-HAP link, r_{h,g_j} denotes the distance from the HAP to the j-th GBS, and Ω_{h,g_j} represents the Nakagami-m fading gain between HAP and the j-th GBS.

4) GBS-LAP mmWave Backhaul Link: The received power at the i-th LAP from the j-th GBS is $P_{r_{l_i,g_j}} = P_{t_g} C_{g,\zeta} G_{t_g} G_{r_l} r_{l_i,g_j}^{-\alpha_{g,\zeta}} \Omega_{l_i,g_j,\zeta}, \zeta \in \{L, N\}$, where G_{r_l} is the mmWave directional gain of the LAP receiver, $C_{g,\zeta}$ and $\alpha_{g,\zeta}$ are the path loss intercept and PLE of the LoS/NLoS GBS-LAP link, r_{l_i,g_j} denotes the distance from the i-th LAP to the j-th GBS, and $\Omega_{l_i,g_j,\zeta}$ represents the Nakagami-m fading gain between i-th LAP and the j-th GBS.

B. Association Rule and Performance Metrics

Each GUE is assumed to connect with the LAP that provides the maximum average received signal strength. We define successful access probability as the probability that the signal-to-interference ratio (SIR) of the access link exceeds a threshold τ_a. The SIR of the user u from its associated LAP l_o can be expressed as $SIR_u = r_l^{-\alpha_{u,\zeta}} \Omega_{l,\zeta} / I_u$, where $I_u = \sum_{i \in \Phi_{l,L}/l_o} r_{l_i,L}^{-\alpha_{l,L}} \Omega_{l_i,L} + \sum_{i \in \Phi_{l,N}/l_o} r_{l_i,N}^{-\alpha_{l,N}} \Omega_{l_i,N}$, and r_l and $\Omega_{l,\zeta}$ are the distance and Nakagami-m fading gain between the typical GUE and its serving LAP l_o, respectively.

Backhaul probability is the probability that the backhaul transmission is successful, i.e., the SNR of the mmWave backhaul link exceeds a threshold τ_b. To establish a reliable and highly directional mmWave link, the transmitter and receiver should align their narrow beams to enhance the intended link and reduce interference before data transmission [13]. As a result, interference is reduced and the mmWave backhaul links become more sensitive to noise. Thus, the signal-to-noise ratio (SNR) is adopted to assess the mmWave backhaul links. The SNR of the LAP l_o from the HAP can be expressed as $SNR_{h,l_o} = P_{t_h} C_h G_{t_h} G_{r_l} r_{l,h}^{-\alpha_h} \Omega_{l,h} / \sigma^2$, where σ^2 represents the noise power. Similarly, the SNR of the HAP and the LAP from the selected backhaul GBS g_o can be expressed as $SNR_{h,g_o} = P_{t_g} C_{g,L} G_{t_g} G_{r_h} r_{h,g}^{-\alpha_{g,L}} \Omega_{h,g} / \sigma^2$ and $SNR_{l_o,g_o} = P_{t_g} C_{g,\zeta} G_{t_g} G_{r_l} r_{l,g}^{-\alpha_{g,\zeta}} \Omega_{l,g} / \sigma^2$.

III. Analytical Results

A. Successful Access Probability

The expression for the successful access probability P_a is derived in Theorem 1.

Theorem 1. *The successful access probability given a successful backhaul link is*

$$P_a = A_L P_{a,L} + A_N P_{a,N}, \tag{1}$$

where A_L is the probability that the typical GUE is associated with a LoS LAP, which is

$$A_L = 1 - \int_0^\infty \exp\left(-2\pi\lambda \int_0^{U_L(x_l)} tP_L(t)dt\right) f_{x_{l,N}}(x_l)dx_l, \tag{2}$$

where $U_L(x_l) = \sqrt{(x_l^2+h_l^2)^{\frac{\alpha_{l,N}}{\alpha_{l,L}}} - h_l^2}$, $f_{x_{l,\zeta}}(x_l) = 2\pi\lambda x_l P_\zeta(x_l)\exp\left(-2\pi\lambda\int_0^{x_l} tP_\zeta(t)dt\right)$, and the probability that the typical GUE is associated with a NLoS LAP is $A_N = 1 - A_L$, and

$$P_{a,\zeta} = \int_0^\infty \sum_{k=0}^{m_{l,\zeta}-1} \frac{s^k}{k!}\left[\frac{\partial^k}{\partial s^k}\mathcal{L}_{I_u,\zeta}(s)\right] f_{x_{l,\zeta}}(x_l)\,dx_l, \tag{3}$$

where $s = m_{l,\zeta}\tau_a(x_l^2+h_l^2)^{\frac{\alpha_{l,\zeta}}{2}}$, and $\mathcal{L}_{I_u,L}(s) = \exp\left(-2\pi\lambda_l\int_x^\infty\left[1-\left(\frac{m_{l,L}}{m_{l,L}+s(x^2+h_l^2)^{-\frac{\alpha_{l,L}}{2}}}\right)^{m_{l,L}}\right]xP_L(x)dx - 2\pi\lambda_l\int_{U_N(x)}^\infty\left[1-\left(\frac{m_{l,N}}{m_{l,N}+s(x^2+h_l^2)^{-\frac{\alpha_{l,N}}{2}}}\right)^{m_{l,N}}\right]xP_N(x)dx\right)$, $\mathcal{L}_{I_u,N}(s) = \exp\left(-2\pi\lambda_l\int_x^\infty\left[1-\left(\frac{m_{l,N}}{m_{l,N}+s(x^2+h_l^2)^{-\frac{\alpha_{l,N}}{2}}}\right)^{m_{l,N}}\right]xP_N(x)dx - 2\pi\lambda_l\int_{U_L(x)}^\infty\left[1-\left(\frac{m_{l,L}}{m_{l,L}+s(x^2+h_l^2)^{-\frac{\alpha_{l,L}}{2}}}\right)^{m_{l,L}}\right]xP_L(x)dx\right)$, $U_N(x) = \sqrt{(x^2+h_l^2)^{\frac{\alpha_{l,L}}{\alpha_{l,N}}} - h_l^2}$.

Proof. Since the GUE connects to the LAP with the maximum average received power, the association probability A_L can be easily derived from $A_L = \mathbb{P}\left(r_l^{-\alpha_{l,L}} > r_{l,N}^{-\alpha_{l,N}}\right)$. Given that the typical GUE is associated with a LoS LAP, the conditional successful access probability can be given by

$$\begin{aligned} P_{a,L} &= \mathbb{E}\left[\mathbb{P}\left(SIR_{u,L} \geq \tau_a \mid x_l\right)\right] \\ &= \int_0^\infty \mathbb{P}\left[\Omega_{l,L} \geq \tau_a I_u (x_l^2+h_l^2)^{\frac{\alpha_{l,L}}{2}} \mid x_l\right] f_{x_{l,L}}(x_l)\,dx_l, \end{aligned} \tag{4}$$

where $f_{x_{l,L}}(x_l) = 2\pi\lambda x_l P_L(x_l)\exp\left(-2\pi\lambda\int_0^{x_l} tP_L(t)dt\right)$ follows the probability density function (PDF) of the conditional horizontal distance x_l separating a typical GUE from its tagged LAP and

$$\begin{aligned} &\mathbb{P}\left[\Omega_{l,L} \geq \tau_a I_u (x_l^2+h_l^2)^{\frac{\alpha_{l,L}}{2}} \mid x_l\right] \\ &\overset{(a)}{=} \mathbb{E}_{I_u}\left[\sum_{k=0}^{m_{l,L}-1}\frac{{I_u}^k}{k!}\left(m_{l,L}\tau_a(x_l^2+h_l^2)^{\frac{\alpha_{l,L}}{2}}\right)^k \right. \\ &\left. \times\exp\left(-m_{l,L}\tau_a(x_l^2+h_l^2)^{\frac{\alpha_l}{2}} I_u\right) \mid x_l\right] \\ &\overset{(b)}{=} \sum_{k=0}^{m_{l,L}-1}\frac{s^k}{k!}\left[\frac{\partial^k}{\partial s^k}\mathcal{L}_{I_{u,L}}(s)\right], \end{aligned} \tag{5}$$

where (a) uses the fact that Ω_l follows a Gamma distribution, and (b) follows the differentiation property of Laplace transform, $s = m_{l,L}\tau_a(x_l^2+h_l^2)^{\frac{\alpha_{l,L}}{2}}$.

$$\begin{aligned} &\mathcal{L}_{I_{u,L}}(s) = \mathbb{E}_{I_u}\left[\exp\left(-sI_u\right)\right] \\ &\overset{(a)}{=} \mathbb{E}_{\Phi_{l,L}}\left[\prod_{i\in\Phi_{l,L}/l_o}\mathbb{E}_{\Omega_{l,L}}\left[\exp\left(-s\Omega_{l,L}(x_{l_i}^2+h_l^2)^{-\frac{\alpha_{l,L}}{2}}\right)\right]\right] \\ &\times\mathbb{E}_{\Phi_{l,N}}\left[\prod_{i\in\Phi_{l,N}/l_o}\mathbb{E}_{\Omega_{l,N}}\left[\exp\left(-s\Omega_{l,N}(x_{l_i}^2+h_l^2)^{-\frac{\alpha_{l,N}}{2}}\right)\right]\right] \\ &\overset{(b)}{=} \mathbb{E}_{\Phi_{l,L}}\left[\prod_{i\in\Phi_{l,L}/l_o}\left(\frac{m_{l,L}}{m_{l,L}+s(x_{l_i}^2+h_l^2)^{-\frac{\alpha_{l,L}}{2}}}\right)^{m_{l,L}}\right] \\ &\times\mathbb{E}_{\Phi_{l,N}}\left[\prod_{i\in\Phi_{l,N}/l_o}\left(\frac{m_{l,N}}{m_{l,N}+s(x_{l_i}^2+h_l^2)^{-\frac{\alpha_{l,N}}{2}}}\right)^{m_{l,N}}\right] \\ &\overset{(c)}{=} e^{-2\pi\lambda_l\int_x^\infty\left[1-\left(\frac{m_{l,L}}{m_{l,L}+s(x^2+h_l^2)^{-\frac{\alpha_{l,L}}{2}}}\right)^{m_{l,L}}\right]xP_L(x)dx} \\ &\times e^{-2\pi\lambda_l\int_{U_N(x)}^\infty\left[1-\left(\frac{m_{l,N}}{m_{l,N}+s(x^2+h_l^2)^{-\frac{\alpha_{l,N}}{2}}}\right)^{m_{l,N}}\right]xP_N(x)dx}, \end{aligned} \tag{6}$$

where (a) follows the i.i.d. distribution of Ω_{l_i} and its further independence from the spatial point process, (b) follows the moment generating function of Gamma distribution, and (c) follows the probability generating functional of the PPP, i.e., $\mathbb{E}\left[\prod_{x\in\Phi} f(x)\right] = \exp\left(-\lambda\int_{\mathbb{R}^2}(1-f(x))\mathrm{d}x\right)$, and we replace x_{l_i} with x. The integration limits can be obtained from the remark below. The conditional successful access probability when the typical GUE is associated with a NLoS LAP can also be obtained following a similar process. □

Remark 1. *Given that the typical GUE is associated with a LoS LAP located at a horizontal distance x, the closest NLoS interferer is at least at a horizontal distance $U_N(x)$. Given that the typical GUE is associated with a NLoS LAP located at a horizontal distance x, the closest LoS interferer is at least at a horizontal distance $U_L(x)$.*

B. Backhaul Probability

A successful backhaul link to the ground core network is essential for a LAP to serve GUE via the aerial link. In the HAB scheme, the backhaul probability is the joint probability that the SNR of HAP-LAP backhaul link and GBS-HAP backhaul link is greater than the backhaul threshold τ_b, i.e. $\mathbb{P}[SNR_{h,l_o} \geq \tau_b, SNR_{h,g} \geq \tau_b] \approx \mathbb{P}[SNR_{h,l_o} \geq \tau_b] \times \mathbb{P}[SNR_{h,g} \geq \tau_b]$. The rationality of the above formula stems from the independence of two events since the two links experience relatively independent channel environment [12]. For simplicity, we use $P_{b,1}$ and $P_{b,2}$ to represent $\mathbb{P}[SNR_{h,l_o} \geq \tau_b]$ and $\mathbb{P}[SNR_{h,g} \geq \tau_b]$.

The backhaul probability of the HAP-LAP link is presented in the following theorem.

Theorem 2. *The backhaul probability $P_{b,1}$ is given by:*

$$P_{b,1} = \int_0^\infty \left[\sum_{k=0}^{m_h-1} \frac{(m_h \tau_b \sigma^2)^k}{k!(P_{t_h} C_h G_{t_h} G_{r_l})^k} (\Delta h^2 + x_l^2)^{\frac{\alpha_h k}{2}} \right] \times \exp\left(\frac{-m_h \tau_b \sigma^2}{P_{t_h} C_h G_{t_h} G_{r_l}} (\Delta h^2 + x_l^2)^{\frac{\alpha_h}{2}} \right) f_{x_l}(x_l)\, dx_l. \tag{7}$$

Proof. Since the HAP is located above the origin, the distance $r_{l,h}$ between the serving LAP and the HAP can be obtained according to the geometry as $r_{l,h} = \sqrt{x_l^2 + \Delta h^2}$, where Δh is the altitude difference between the HAP and LAP layer. Therefore, the backhaul probability $P_{b,1}$ can be derived as:

$$\begin{aligned} P_{b,1} &= \mathbb{E}\left[\mathbb{P}\left(SNR_{h,l_o} \geq \tau_b \mid x_l\right)\right] \\ &= \int_0^\infty \mathbb{P}\left[\Omega_{h,l} \geq \frac{\tau_b \sigma^2 (\Delta h^2 + x_l^2)^{\frac{\alpha_h}{2}}}{P_{t_h} C_h G_{t_h} G_{r_l}} \mid x_l \right] f_{x_l}(x_l)\, dx_l \\ &= \int_0^\infty \left[\sum_{k=0}^{m_h-1} \frac{(m_h \tau_b \sigma^2)^k}{k!(P_{t_h} C_h G_{t_h} G_{r_l})^k} (\Delta h^2 + x_l^2)^{\frac{\alpha_h k}{2}} \right] \\ &\times \exp\left(\frac{-m_h \tau_b \sigma^2}{P_{t_h} C_h G_{t_h} G_{r_l}} (\Delta h^2 + x_l^2)^{\frac{\alpha_h}{2}} \right) f_{x_l}(x_l)\, dx_l. \end{aligned} \tag{8}$$

□

From Theorem 2, we can see that the LAP density and aerial platform heights would affect the backhaul performance. Then we start to derive the backhaul probability of GBS-HAP link. Considering the constraint that the available GBSs are outside disc D, we first derive the PDF of the horizontal distance x_g from HAP to the nearest available GBS.

Lemma 1. *The PDF of x_g is given by:*

$$f_{x_g}(x_g) = \begin{cases} e^{-\lambda_g \pi ({x_g}^2 - {r_d}^2)} 2\pi \lambda_g x_g, & x_g > r_d \\ 0, & \textit{otherwise.} \end{cases} \tag{9}$$

Proof. The PDF of x_g can be derived using the fact that the null probability of a PPP in an area A is $\exp(-\lambda A)$, where λ is the intensity of the PPP. Therefore the CDF of x_g can be given by:

$$F_{x_g}(x_g) = 1 - \exp(-\lambda_g S(x_g)), \tag{10}$$

where $S(x_g)$ is the area of the region and $S(x_g) = \pi {x_g}^2 - \pi {r_d}^2$ when $x_g > r_d$ and $S(x_g) = 0$ otherwise. Finally, the PDF of x_g can be obtained by $f_{x_g}(x_g) = dF_{x_g}(x_g)/dx_g$. □

Theorem 3. *The backhaul probability $P_{b,2}$ is given by:*

$$P_{b,2} = \int_{r_d}^\infty \left[\sum_{k=0}^{m_{g,L}-1} \frac{(m_{g,L} \tau_b \sigma^2)^k}{k!(P_{t_g} C_{g,L} G_{t_g} G_{r_h})^k} (h_h^2 + x_g^2)^{\frac{\alpha_{g,L} k}{2}} \right] \times \exp\left(\frac{-m_{g,L} \tau_b \sigma^2}{P_{t_g} C_{g,L} G_{t_g} G_{r_h}} (h_h^2 + x_g^2)^{\frac{\alpha_{g,L}}{2}} \right) f_{x_g}(x_g)\, dx_g, \tag{11}$$

where $f_{x_g}(x_g)$ is given in Lemma 1.

Proof. Similar to the proof of Theorem 2. □

In the LDB scheme, the backhaul probability $P_{b,l}$ can be obtained by the modification of Theorem 1 in [12]. The complete expression is omitted due to space limitation.

TABLE I
MAIN PARAMETERS

Parameters	Values
Radius of malfunction area	20 km
Altitude of HAP h_h	18 km
Transmit power P_{t_l}, P_{t_h}, P_{t_g}	25 dBm, 30 dBm, 37 dBm
PLE $\alpha_{l,L}$, $\alpha_{l,N}$, α_h, $\alpha_{g,L}$, $\alpha_{g,N}$	2.5, 3, 2.05, 2.5, 2.5, 3
Path loss intercept C_h, $C_{g,L}$, $C_{g,N}$	-69.8 dB, -69.8 dB, -69.8 dB
Nakagami-m parameter $m_{l,L}$, $m_{l,N}$, m_h, $m_{g,L}$, $m_{g,N}$	2, 1, 2, 2, 1
Antenna gain G_{t_h}, G_{t_g},G_{r_l}, G_{r_h}	10, 10, 10, 10
Noise power σ^2	-130 dBm
Density of LAPs and GBSs λ_l, λ_g	0.2 /km^2, 10 /km^2
Access and backhaul threshold τ_a, τ_b	-10 dB, 0 dB

C. Coverage Probability

The overall coverage probability is the joint probability of successful access and backhaul. After deriving the access probability in Eq. (3) and the backhaul probabilities in Eq. (7) and Eq. (11), the overall coverage probability $P_{cov,h}$ in the HAB scheme can be obtained as $P_{cov,h} = P_a \times P_{b,1} \times P_{b,2}$, while the overall coverage probability $P_{cov,l}$ in the LDB scheme can be obtained as $P_{cov,l} = P_a \times P_{b,l}$

IV. Numeric Results and Discussions

This section presents the numeric results obtained from the proposed analytical framework and validated through Monte Carlo simulations. The HAB scheme is numerically evaluated against the LDB scheme and ideal backhaul (IB) scheme in which the backhaul impact is not taken into consideration. Unless otherwise stated, the values of main parameters are given in Table. I. The settings of simulation parameter values mainly refer to references [4] and [12].

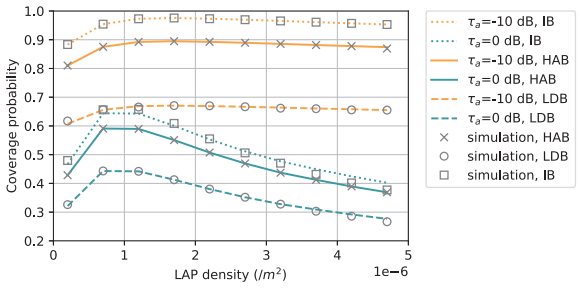

Fig. 2. Coverage probability as function of the LAP density for different access threshold.

Fig. 2 explores how the density of LAPs impacts the coverage probability for h_l = 100 m for different access thresholds τ_a. The performance gap between the IB scheme and the other two schemes shows the error caused by not considering the backhaul constraints. It can be seen that increasing the density of LAPs first improves the coverage probability but then deteriorates it. For low LAP densities, the distance between GUE and its neighboring LAP can be closer as the LAP density increases, which brings lower path loss and thus harvest a better access probability. The backhaul probability also tends to increase slightly as the LAP density increase because the distance between LAPs and HAP/GBSs can be

lower. However, the added LAPs bring higher interference levels and the negative effect becomes the dominant factor when the LAP density exceeds a certain bound, which leads to deterioration of coverage probability.

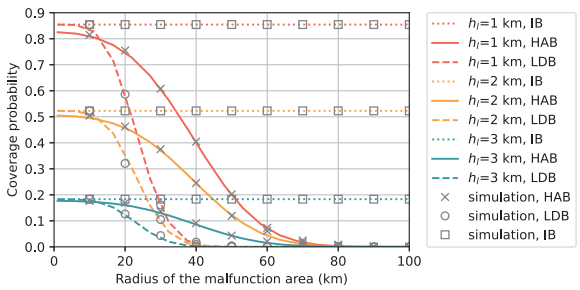

Fig. 3. Coverage probability as function of the malfunction area radius for different LAP altitudes.

Then we compare the performance of these schemes under different malfunction area radius and different LAP heights in Fig. 3. The radius of the malfunction area does not affect the access probability, but only the backhaul probability, so the coverage probability of the IB scheme is a straight line. The gap between coverage probability lines of IB scheme shows the impact of LAP height on access link. For higher LAP altitudes, the access probability reduces since longer distance brings more attenuation. With the increase of the malfunction area radius, the LDB scheme can be effective at first, but it becomes very difficult for LAPs to directly backhaul to the ground when a large range of GBSs are not available. Limited by the backhaul capability, the coverage performance of LDB scheme deteriorates sharply in large-scale disaster scenarios while the HAB scheme performs better. The intersection of two curves of HAB and LDB represents the condition when the two schemes achieve equal performance. We call the abscissa value of the intersection as the critical malfunction area radius. To better observe the relationship between aerial platform altitude and critical malfunction area radius, we present Fig. 4.

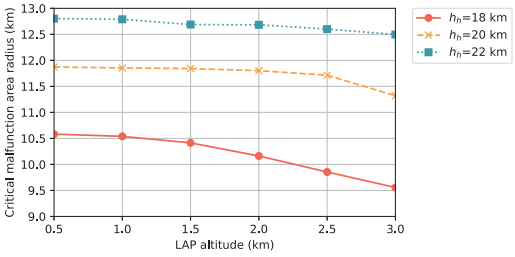

Fig. 4. Critical malfunction area radius when HAB and LDB have equal coverage performance.

The curves in Fig. 4 indicate that under the current situation, HAB and LDB can achieve equal coverage performance. The area below the curve should adopt the LDB scheme, while it is better for the upper part of the curve to adopt the HAB scheme. For example, when the HAP and LAPs operate at 20 km and 500 m respectively, we recommend the HAB scheme if the malfunction area radius exceeds 11.87 km. In practical implementation, an appropriate backhaul scheme can be selected according to the malfunction area radius and the available deployment altitude of aerial platforms to obtain better coverage. When the malfunction area exceeds a certain bound, it is necessary to deploy a HAP to assist the backhaul of LAPs to provide better services for GUE.

V. Conclusion

This letter utilizes stochastic geometry to derive an analytical framework for coverage analysis of the IHL system considering backhaul constraints. Based on the proposed analytical framework, the impacts of key parameters, such as aerial platform altitudes and LAP densities, on network performance are studied. Results show that HAB scheme obtains better performance compared to LDB scheme when the malfunction area radius is larger than a certain bound. This work can be expected as a pioneer theoretically guiding network operators to properly design backhaul of LAP aerial base stations in the emergency response of post-disaster malfunction areas.

References

[1] M. Matracia, M. A. Kishk, and M.-S. Alouini, "On the topological aspects of UAV-assisted post-disaster wireless communication networks," *IEEE Communications Magazine*, vol. 59, no. 11, pp. 59–64, 2021.

[2] Y. Zhu, W. Bai, M. Sheng, J. Li, D. Zhou, and Z. Han, "Joint UAV access and GEO satellite backhaul in IoRT networks: Performance analysis and optimization," *IEEE Internet of Things Journal*, vol. 8, no. 9, pp. 7126–7139, 2021.

[3] X. Cao, P. Yang, M. Alzenad, X. Xi, D. Wu, and H. Yanikomeroglu, "Airborne communication networks: A survey," *IEEE Journal on Selected Areas in Communications*, vol. 36, no. 9, pp. 1907–1926, 2018.

[4] J. Qiu, D. Grace, G. Ding, M. D. Zakaria, and Q. Wu, "Air-ground heterogeneous networks for 5G and beyond via integrating high and low altitude platforms," *IEEE Wireless Communications*, vol. 26, no. 6, pp. 140–148, 2019.

[5] G. Karabulut Kurt, M. G. Khoshkholgh, S. Alfattani, A. Ibrahim, T. S. J. Darwish, M. S. Alam, H. Yanikomeroglu, and A. Yongacoglu, "A vision and framework for the high altitude platform station (HAPS) networks of the future," *IEEE Communications Surveys Tutorials*, vol. 23, no. 2, pp. 729–779, 2021.

[6] M. Helmy and H. Arslan, "Utilization of aerial heterogeneous cellular networks: Signal-to-interference ratio analysis," *Journal of Communications and Networks*, vol. 20, no. 5, pp. 484–495, 2018.

[7] Z. Jia, Q. Wu, C. Dong, C. Yuen, and Z. Han, "Hierarchical aerial computing for Internet of Things via cooperation of HAPs and UAVs," *IEEE Internet of Things Journal*, pp. 1–1, 2022.

[8] Y. Du, K. Wang, K. Yang, and G. Zhang, "Trajectory design of laser-powered multi-drone enabled data collection system for smart cities," in *2019 IEEE Global Communications Conference (GLOBECOM)*, 2019, pp. 1–6.

[9] D. Wang, Y. He, K. Yu, G. Srivastava, L. Nie, and R. Zhang, "Delay sensitive secure NOMA transmission for hierarchical HAP-LAP medical-care IoT networks," *IEEE Transactions on Industrial Informatics*, pp. 1–1, 2021.

[10] H. Ahmadinejad and A. Falahati, "Forming a two-tier heterogeneous air-network via combination of high and low altitude platforms," *IEEE Transactions on Vehicular Technology*, vol. 71, no. 2, pp. 1989–2001, 2022.

[11] C. K. Armeniakos and A. G. Kanatas, "Performance comparison of wireless aerial 3D cellular network models," *IEEE Communications Letters*, vol. 26, no. 8, pp. 1779–1783, 2022.

[12] N. Kouzayha, H. ElSawy, H. Dahrouj, K. Alshaikh, T. Y. Al-Naffouri, and M.-S. Alouini, "Stochastic geometry analysis of hybrid aerial terrestrial networks with mmWave backhauling," in *ICC 2020 - 2020 IEEE International Conference on Communications (ICC)*, 2020, pp. 1–7.

[13] N. Michelusi and M. Hussain, "Optimal beam-sweeping and communication in mobile millimeter-wave networks," in *2018 IEEE International Conference on Communications (ICC)*, 2018, pp. 1–6.